

## ANALYSIS OF EUV, MICROWAVE, AND MAGNETIC FIELD OBSERVATIONS OF SOLAR PLAGE

J W BROSIUS, J M DAVILA, H P JONES, W T THOMPSON,  
R J THOMAS, G D HOLMAN  
NASA Goddard Space Flight Center, Code 682, Greenbelt, MD 20771

S M WHITE, N GOPALSWAMY, M R KUNDU  
Astronomy Program, University of Maryland, College Park, MD 20742

**ABSTRACT** We obtained simultaneous images of solar plage on 7 May 1991 with Goddard Space Flight Center's Solar EUV Rocket Telescope and Spectrograph (SERTS), the Very Large Array (VLA), and the NASA/NSO spectromagnetograph at Kitt Peak. Using intensity ratios of Fe XVI to Fe XV emission lines, we find that the coronal plasma temperature is  $2.5 \pm 0.3 \times 10^6$  K throughout the region. The column emission measure ranges from  $2.6 \times 10^{27}$  to  $1.3 \times 10^{28}$  cm<sup>-5</sup>. The calculated structure and intensity of the 20 cm wavelength thermal bremsstrahlung emission from the hot plasma observed by SERTS is quite similar to the observed structure and intensity of the 20 cm microwave emission observed by the VLA. Using the revised coronal iron abundance of Meyer (1991, 1992), we find no evidence for either cool absorbing plasma or for contributions from thermal gyroemission. Combining the observed microwave polarization and the SERTS plasma parameters, we calculate a map of the coronal longitudinal magnetic field. The resulting values,  $\sim 30 - 60$  Gauss, are comparable to extrapolated values of the potential field at heights of 5,000 and 10,000 km.

## INTRODUCTION

Simultaneous observations of the Sun in the X-ray, EUV, optical, and microwave bands provide a wealth of information concerning the plasma and magnetic field in the solar corona. This information is vital to understanding processes such as coronal heating, solar wind acceleration, pre-flare energy storage, and active region evolution.

Using temperature-sensitive EUV ionic emission line intensity ratios, the coronal plasma electron temperature can be determined. Combining this temperature with the emission line intensity, the column emission measure can also be determined. These quantities are not only important by themselves, but are also essential ingredients for determining the coronal magnetic field strength. Because Zeeman splitting in coronal emission lines is undetectable, the Zee-

man effect cannot be used for measuring the coronal magnetic field strength. A different method for obtaining this measurement is made possible by virtue of the dependence of the microwave emission upon the coronal magnetic field strength. It is accomplished using the combined set of multiwaveband observations as described below (see also Brosius et al. 1992a, Webb et al. 1987, Lang et al. 1987, and references therein).

## OBSERVATIONS AND DATA ANALYSIS

The SERTS imaging spectrograph is described by Neupert et al. (1992). The instrument incorporates an imaging fore-optic with its image plane at the entrance aperture of a toroidal grating spectrograph. The spectrograph entrance aperture is designed so that spectra are obtained along a slit connecting two rectangular lobes. Monochromatic images are obtained in the lobes.

SERTS acquired spectrographic data between 235 and 450 Å from 1806 to 1813 UT on 7 May 1991 (Davila et al. 1992). The relative intensities are accurate to better than 20% at wavelengths above 300 Å, and are somewhat worse at wavelengths below 300 Å. The absolute photometric scale, accurate to better than a factor of 2, was derived by fitting our solar observations to reported values for the average He II quiet sun flux at 304 Å (Thomas, Neupert, & Thompson 1991). The uncertainty in the absolute photometric scale means that derived column emission measures are uncertain by factors approaching 2.

The SERTS observations were coaligned with the Kitt Peak and VLA observations by matching features common to both the SERTS He II 304 Å image and the Kitt Peak He I 10830 Å image. Because the pointing of the VLA relative to Kitt Peak is known, the coalignment of the SERTS images relative to Kitt Peak images yields a mutually coaligned data set.

Table I lists typical intensities in six prominent emission lines for which images of solar plage located at N11W10 have been obtained. Also listed are wavelength and temperature of maximum emissivity. Notice that the ratios of the intensities of the Fe XVI lines at 361 and 335 Å (0.51) and of the Fe XV lines at 417 and 284 Å (0.036) are in excellent agreement with their respective density- and temperature-independent theoretical ratios of 0.48 and 0.034.

TABLE I Intensities of plage emission lines in  $\text{ergs cm}^{-2} \text{s}^{-1} \text{sr}^{-1}$

ion	$\lambda(\text{Å})$	$T^{\text{max}}(\text{K})$	$I_{\text{avg}}$	$I_{\text{min}}$	$I_{\text{max}}$
He II	303.784	$5.0 \times 10^4$	$9.63 \times 10^3$	$4.20 \times 10^3$	$2.67 \times 10^4$
Mg IX	368.067	$1.0 \times 10^6$	$1.14 \times 10^3$	$5.77 \times 10^2$	$2.44 \times 10^3$
Fe XV	284.158	$2.0 \times 10^6$	$8.92 \times 10^3$	$4.85 \times 10^3$	$1.45 \times 10^4$
Fe XV	417.245	$2.0 \times 10^6$	$3.17 \times 10^2$	$1.72 \times 10^2$	$5.69 \times 10^2$
Fe XVI	335.401	$2.5 \times 10^6$	$4.44 \times 10^3$	$1.92 \times 10^3$	$1.09 \times 10^4$
Fe XVI	360.754	$2.5 \times 10^6$	$2.26 \times 10^3$	$1.02 \times 10^3$	$4.99 \times 10^3$

The NASA/NSO Spectromagnetograph was used to obtain a photospheric longitudinal magnetogram and a He I 10830 Å image. A filament channel straddles the neutral line separating the two main regions of opposite magnetic polarity. On one side of this channel, a small region of strong positive magnetic polarity is spaced closely with regions of strong negative magnetic polarity. The EUV intensities peak at this location.

Observations were made in the 20 cm waveband with the D-configuration VLA. Maps were made separately in the left hand (L) and right hand (R) modes of circular polarization. Emission in these components is commonly expressed in terms of brightness temperature ( $T_B^R$  and  $T_B^L$ , in K), which is the blackbody temperature corresponding to the measured flux density at the observed microwave wavelength. For an optically thick source, the brightness temperature of the emerging radiation is equal to the electron temperature of the source. Total intensity (Stokes I) is  $\frac{1}{2}[T_B^R + T_B^L]$ , and the degree of circular polarization (Stokes V) is  $\frac{1}{2}[T_B^R - T_B^L]$ . The fractional polarization is given by V/I. The intensity shows a two-peaked structure, one peak on each side of the filament channel, with a weak bridge of emission connecting the two.

## RESULTS

For this analysis, we use the intensities of Fe XVI ( $\text{Fe}^{+15}$ ) at 335 Å ( $I_{335}$ ) and Fe XV ( $\text{Fe}^{+14}$ ) at 284 Å ( $I_{284}$ ). Using standard procedures for calculating the rates of emission per unit volume for collisionally excited ionic emission lines (e.g., Stern, Wang, & Bowyer 1978; Landini & Monsignori Fossi 1990), and combining the ionization equilibrium calculations of Arnaud & Raymond (1992) with the relevant atomic physics parameters, we obtain a simple expression relating the line intensity ratio  $I_{335}/I_{284}$  to the electron temperature. The resulting map shows little variability across the plage, with a maximum value of  $2.8 \times 10^6$  K, a minimum value of  $2.2 \times 10^6$  K, and a typical value of  $2.5 \times 10^6$  K. By combining the temperature map and one of the EUV intensity maps used to obtain this temperature map, and using the revised Meyer (1991, 1992) coronal iron abundance, a map of the column emission measure ( $EM = \int N_e^2 dl$ ) is obtained. The emission measure ranges from  $2.6 \times 10^{27}$  to  $1.3 \times 10^{28}$  cm<sup>-5</sup>.

Electron temperature and column emission measure maps obtained from the EUV data were used to compute the 20 cm thermal bremsstrahlung intensity. Because this map, calculated for the hot coronal plasma observed by SERTS, yields both the structure and the brightness temperature observed with the VLA, we conclude that thermal bremsstrahlung from this hot plasma alone is the mechanism responsible for the observed microwave emission. Neither cool absorbing plasma nor magnetic fields sufficient to produce gyroemission are required in the corona over the plage.

Combining the plasma parameters obtained using SERTS with the microwave polarization obtained using the VLA, we calculated a map of the coronal longitudinal magnetic field  $B_z$ . This is possible because of the dependence of the thermal bremsstrahlung optical depth upon the coronal magnetic field. Careful attention has been given to relating each mode of circular polarization (R or L) with its appropriate mode of propagation (extraordinary or ordinary) to obtain the direction of the magnetic field in the microwave emission region.

For comparison we calculated maps of the extrapolated coronal potential longitudinal magnetic field at heights of 5,000 and 10,000 km using the Sakurai (1982) code. Our calculated values from the combined SERTS and VLA observations are consistent with the extrapolated potential values. These results are described in more detail in a recent paper by Brosius et al. (1992b).

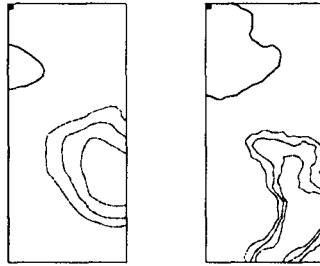


Fig. 1. Coronal longitudinal magnetic field (left) calculated with SERTS and VLA observations, and (right) extrapolated from the photospheric magnetogram to a height of 10,000 km. Contours are +10 (solid), -30, -40, -50 (dotted) Gauss. Rectangles are  $106'' \times 230''$ . Solar north is  $50^\circ$  clockwise from the top.

### ACKNOWLEDGEMENTS

This work was supported in part by NASA RTOPs 170-38-53 and 879-11-38. The VLA is an NRAO facility, operated by Associated Universities, Inc., under cooperative agreement with NSF. NSO/Kitt Peak data used here are produced cooperatively by NSF/NOAO, NASA/GSFC, and NOAA/SEL.

### REFERENCES

- Arnaud, M., & Raymond, J. 1992, *ApJ* **398**, 394  
 Brosius, J.W., Willson, R.F., Holman, G.D., & Schmelz, J.T. 1992a, *ApJ* **386**, 347  
 Brosius, J.W., et al. 1992b, *ApJ*, submitted  
 Davila, J.M., Thomas, R.J., Thompson, W.T., Keski-Kuha, R.A.M., & Neupert, W.M. 1992, in *Proc. 10th Colloq. on UV & X-Ray Spect.*, in press  
 Landini, M., & Monsignori Fossi, B.C. 1990, *A&AS* **82**, 229  
 Lang, K.R., Willson, R.F., Smith, K.L., & Strong, K.T. 1987, *ApJ* **322**, 1035  
 Meyer, J.-P. 1991, *Adv. Space Res.* **11**, 269  
 Meyer, J.-P. 1992, private communication  
 Neupert, W.M., Epstein, G.L., Thomas, R.J., & Thompson, W.T. 1992, *Sol. Phys.* **137**, 87  
 Sakurai, T. 1982, *Sol. Phys.* **76**, 301  
 Stern, R., Wang, E., & Bowyer, S. 1978, *ApJS* **37**, 195  
 Thomas, R.J., Neupert, W.M., & Thompson, W.T. 1991, *BAAS* **23**, 1387  
 Webb, D.F., Holman, G.D., Davis, J.M., Kundu, M.R., & Shevgaonkar, R.K. 1987, *ApJ* **315**, 716